POOL BOILING HEAT TRANSFER FROM HORIZONTAL TUBES TO ALTERNATIVE REFRIGERANTS

D. GORENFLO
Laboratorium für Wärme- und Kältetechnik
Universität -GH- Paderborn, Germany

ABSTRACT

Pool boiling heat transfer from single plain tubes with widely differing diameters, from single finned tubes with enhanced surfaces, and the heat transfer caused by the additional convection of the bubbles and liquid streaming upwards within a tube bundle have been investigated experimentally. The boiling liquids are propane, n-butane, n-hexane, propane/n-butane mixtures, and the partly fluorinated refrigerants R134a, R152a, a mixture of R134a/R152a and R227.

The results show that the influence of the tube diameter on nucleate boiling heat transfer is much smaller than could be concluded from some of the sources in the literature, if the surface roughness and the wall material of the tubes compared are exactly the same. Roughly speaking, there is practically no influence at intermediate heat fluxes over a wide pressure range, while a big diameter is favourable at small fluxes and low pressures, and it is at a disadvantage at high fluxes and high pressures.

The finned tubes with enhanced surfaces augment the heat transfer rate per tube length significantly over plain tubes, especially at saturation pressures lower than thirty per cent of the critical pressure and at small to intermediate heat fluxes.

The additional convection caused by the vapour bubbles and the liquid streaming upwards within the tube bundle of a shell-and-tube evaporator may increase the heat transfer coefficients at low heat fluxes drastically, if the saturation pressures are not very high. This holds above all for the boiling of mixtures, where the well known deterioration of heat transfer against the molar average of the heat transfer coefficients of the pure components may be compensated or even overcompensated.

1 INTRODUCTION

Connecting pool boiling heat transfer with alternative refrigerants we have in mind above all compression cycles with evaporation and condensation in refrigerating machines, and hence the *alterntive refrigerants* will be pure or partly fluorinated hydrocarbons to replace the fully substituted CFC's. Their heat transfer performance is similar to that of the relevant groups of substances, e.g. hydrocarbons or halocarbons, resp..

Despite the much research effort which has been devoted to pool boiling heat transfer in the past, no coherent theory yet exists that would allow heat transfer coefficients during nucleate pool boiling to be predicted to within the accuracy required in engineering. Thus, at the current state of the art, only empirical or semiempirical correlations can be applied in practice. The expositions of this paper will be mainly focussed on improving this kind of correlations. In this context, new experimental results will be presented on the following topics:

- Pool boiling heat transfer from single plain tubes with different diameters to propane and n-hexane in a wide range of heat fluxes and saturation pressures.
- Pool boiling heat transfer at single finnned high flux tubes with different fin shapes. Boiling liquids: R134a; R152a; a nearly equimolar mixture of R134a/R152a; propane.
- Convective effects on pool boiling heat transfer within tube bundles, simulated by vapour bubbles or liquid flowing upwards to a single tube with big diameter ($D \approx 88$ mm). Boiling liquids: Propane, n-butane, n-hexane, and two propane/n-butane mixtures with approx. 25 or 50 mole% propane.

The experimental setups used are modified versions of the so-called Standard Apparatus for pool boiling heat transfer measurements (c.f. eg./1/,/2/). The main features are:

- natural circulation loop between evaporator and condenser,
- dc-heated, horizontal test tube within the evaporator and
- insulated box surrounding the whole loop, the air temperature of which is thoroughly adjusted to the saturation temperature T_s of the pool of liquid in the evaporator.

Modifications for simulating convective effects within tube bundles:

- U-shaped additional heating tube, 50 mm below the test tube, with 6.5 mm O.D. for additional flow of bubbles from below and
- distributing tube for additional flow of liquid from below, fed by a gear pump with speed regulation and a maximum discharge capacity of 9 litres per minute.

2 POOL BOILING HEAT TRANSFER FROM SINGLE PLAIN TUBES WITH DIFFERENT DIAMETERS

The experiments presented in this chapter aim at enlarging the knowledge existing in the literature /3/-/9/ about the influence of the diameter of horizontal evaporator tubes on pool boiling heat transfer. A big tube with 88.4 mm O.D. has been chosen as test tube to get clear evidence of the effects. The boiling liquids are propane at high saturation pressures (10 to 80% of the critical pressure), and n-hexane at low (10 to approx. 1% of the critical pressure). The purity is better than 99.5 vol-%. The heat flux varies from beginning nucleation (100 W/m^2) up to very intense nucleate boiling (~ 70 000 W/m^2). For comparison, corresponding results of a tube with 7.6 mm O.D. and with the same wall material and surface roughness will also be discussed /10/.

The surface of the test tube has been emery ground by a mechanical device in exactly the same manner as the surface of the small tube before. The main roughness parameters according to German standards are given in Table I, showing that the roughness structures of the two surfaces should be quite similar.

TABLE I: Roughness parameters of the tube surfaces according to the German Standards 4762 or 4768, resp.. Tube material: Mild Steel St 35.8

Tube	Surface roughness* (µm) R_a	R_q	R_p	R_z	number of measurements
D = 88.4 mm	0.18	0.23	0.63	1.13	80
D = 7.6 mm	0.20	0.26	0.68	1.16	18

*The figures are mean values of measurements at various positions on the test tube surface (preferably above the thermocouples in the wall).

Figure 1 shows double logarithmic plots of the heat transfer coefficient α over the heat flux q for propane and n-hexane boiling on the outside of the plain tube with 88.4 mm O.D. at different normalized saturation pressures $p^* = p_s/p_c$ (p_c = critical pressure).

α is defined by the ratio of the heat flux q and the *mean* superheat ΔT of the tube wall surface over the saturation temperature T_s of the boiling liquid (q and ΔT are calculated assuming only *radial* heat flow to the surface)

$$\alpha = q/\Delta T = q/(T_{Wall} - T_s) \qquad (1).$$

The heat transfer coefficient increases with rising heat flux and pressure, as is well known from the literature for tubes with small diameters (cf.eg./11).. At constant pressure, α can be interpolated quite well by straight lines in this kind of plot, thus

$$\alpha \sim q^n \qquad (2),$$

except at the highest pressures and heat fluxes, where the increase diminishes somewhat, see the upper diagram. At low pressures and small fluxes, free convective heat transfer occurs without bubble formation, the α-values following the correlation for turbulent flow /11/ (except two measurements with hexane at $p^* = 0.12$),

$$Nu = 0.15\ (Gr \cdot Pr)^{1/3} \quad (\text{or } \alpha \sim q^{1/4}) \qquad (3),$$

where Nu = Nusselt, Gr = Grashof and Pr = Prandtl number, and the characteristic length = tube diameter D in Nu and Gr (getting eliminated in eq(3), as Nu ~ D and Gr ~ D^3).

Figure 2 contains the comparison of the two tubes at selected pressures within the whole range investigated. ***At low heat fluxes***, the big tube (full lines) is superior to the small (dashed lines), the effect being most pronounced at intermediate pressures, $0.1 \leq p^* \leq 0.03$, corresponding to approx. $4 \leq p_s \leq 1$ bar, and tending to vanish towards higher and lower pressures. As it will be shown in detail in Chapt.3, the improvement is caused by the bubbles on the lower parts of the tube surface; it decreases towards *lower* pressures, because the number of growing and rising bubbles gets smaller within the regime of beginning nucleation, and it vanishes at *high* pressures, because many

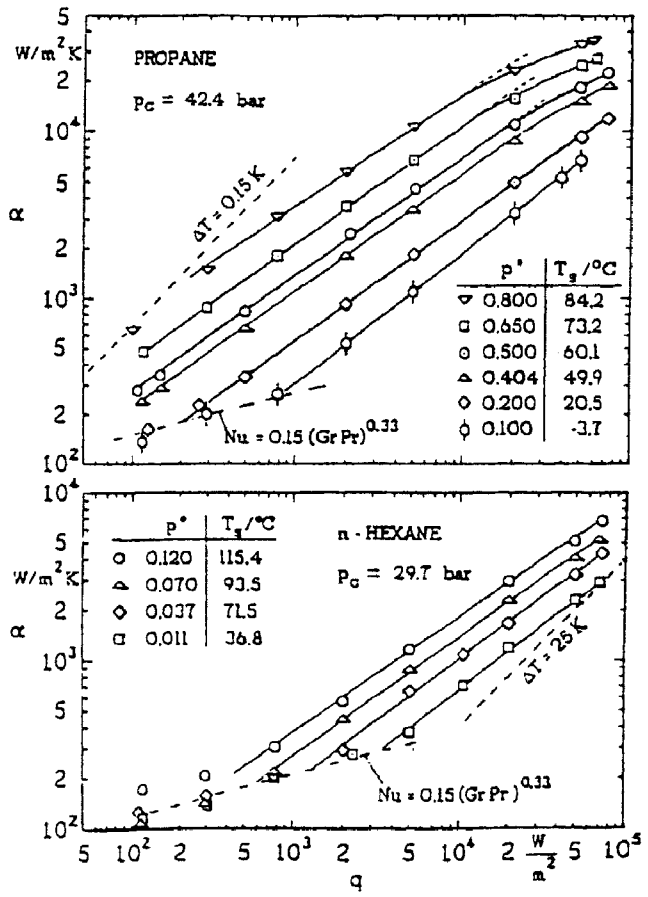

Fig. 1: Double logarithmic plots of the heat transfer coefficient α as function of the heat flux q for propane (top) and n-hexane (bottom) boiling at the tube with 88.4 mm O.D. and emery ground surface. Tube material: Mild steel St35.8

tiny bubbles are created by nucleation all over the tube surface - even at very small superheats - and because buoyancy diminishes rapidly for two reasons: smaller bubbles and smaller vapour/liquid density difference.

At constant pressure and ***Increasing heat flux***, the improvement of the big tube over the small also vanishes because of the dense layer of bubbles produced on the heated surface by nucleation, and beginning at approx. 20% of the critical pressure the greater number of bubbles streaming upwards at the big tube rather exhibit an additional resistance to the replacement of the liquid at the tube surface and therefore to the heat transfer.

Very recent measurements of Hahne et al /12/ for nucleate boiling of propane at a thin horizontal platinum wire (D = 0.1 mm) have been added as closed circles in the upper diagram of Fig.2. The data are in good agreement with the results of the tubes at the same normalized saturation pressure $p^* = 0.1$.

In Fig.3, the dependences of the heat transfer coefficient from heat flux and saturation pressure are represented by the exponent n of the proportionality (2) (upper diagram) and by α-values which have been interpolated at two constant heat fluxes (20 000 and 2 000 W/m^2) and normalized to the values α_o at $p_o^* = 0.1$ for the two liquids and the two fluxes (lower diagrams). The exponents n for the big tube (open symbols) agree quite well with the values for the small (partly closed symbols) at high pressures, while they are significantly smaller at low pressures, especially in the case of hexane (squares). All the data lie within the limit of scatter valied for the function

$$n(p^*) = 0.9 - 0.3\ p^{*0.3} \qquad (4)$$

as given by the VDI-Heat Atlas /11/. Eq(4) was deduced from a great number of measurements with hydrocarbons, refrigerants and other liquids in the literature. Like here, several recent experimental papers for tubes with small diameters report somewhat higher

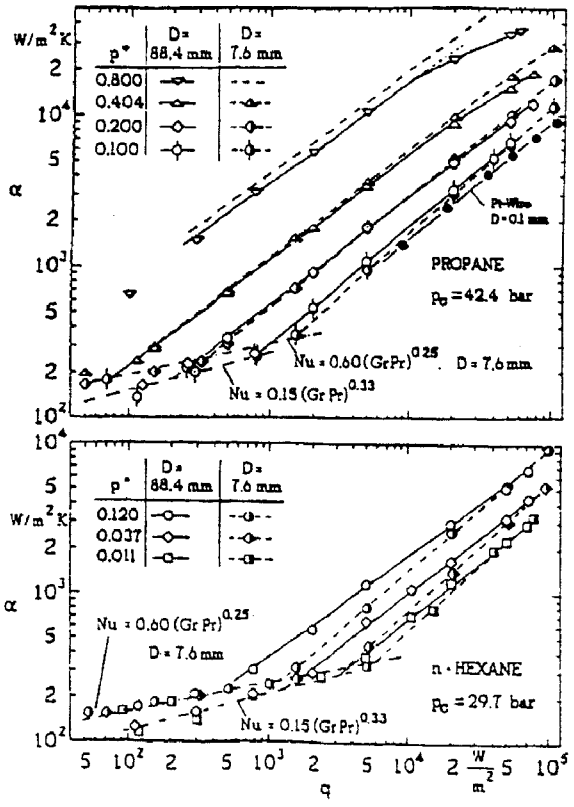

Fig.2: Comparison of the results for propane (top) and n-hexane (bottom) boiling at two tubes with different diameters and the same surface roughness and wall material (mild steel St35.8). In addition: Data for propane at $p^* = p/p_c = 0.1$ boiling at a Pt-wire of 0.1 mm diameter (closed circles, top) /12/.

n-values than predicted by eq(4), cf. the survey in /10/. The exponent n for the wire (closed circle in the diagram on top) is in good agreement with eq(4), as had also been found by Shi et al. for other refrigerants /13/.

From the lower diagrams of Fig.3, it can be seen that the relative pressure dependence of α is quite similar for the two tubes and can be well correlated by /11/

$$\frac{\alpha}{\alpha_{o,q=20\,000}} = F(p^*) = 1.2\ p^{*0.27} + 2.5\ p^* + \frac{p^*}{1-p^*} \qquad (5)$$

or

$$\frac{\alpha}{\alpha_{o,q=2\,000}} = F(p^*) \cdot 0.1^{n(p^*) - n(p_o^*)} \qquad (5a).$$

The pressure dependence for the small tube (extrapolated to high pressures (+) by measurements in /10/) is somewhat stronger than predicted by eq(5), whereas the measurements of Shi et al /13/ with the platinum wire correspond with the VDI-Heat Atlas correlation as well as the data for the big tube, at least *at high heat fluxes.*

As a conclusion of this chapter, the results show that the tube diameter has but little influence on the heat transfer coefficient α at nucleate pool boiling, if the circumferentially averaged superheat ΔT of the tube wall is used in the definition of α (eq(1)): A big diameter is favourable at small fluxes and low pressures, while it is at a disadvantage at high fluxes and high pressures. At intermediate heat fluxes, there is almost no influence over a wide pressure range. The latter holds even for the data of the platinum wire, as will be explained in detail elsewhere /14/.

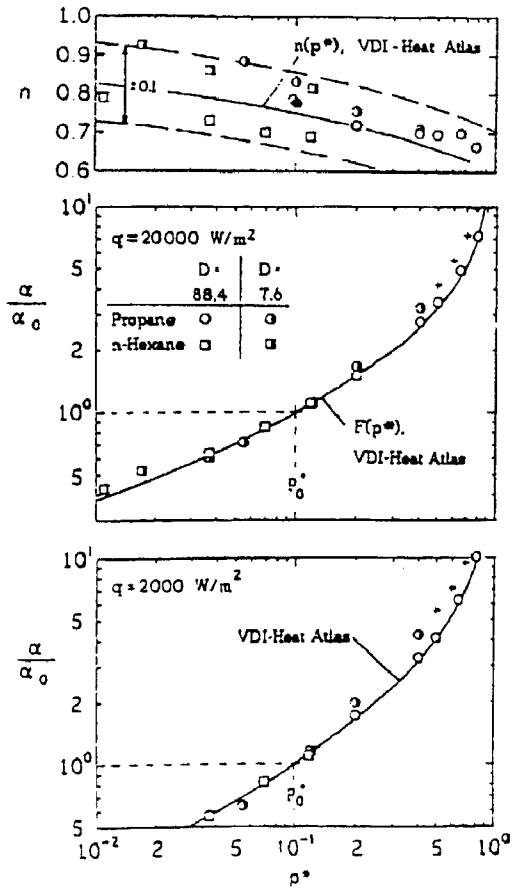

Fig.3: Relative pressure dependences of the exponent n (top) and of the heat transfer coefficients interpolated at two heat fluxes and normalized to the respective values α_o at $p_o^* = 0.1$

Full lines: Calculation method of the VDI-Heat Atlas /11/.
Crosses: Extrapolation according to results for copper tubes (D = 8 mm) /10/.
Closed circle: Propane boiling at a Pt-wire /12/ (diagram on top).

3 POOL BOILING HEAT TRANSFER AT SINGLE FINNED HIGH FLUX TUBES

Pool boiling heat transfer from single horizontal plain and finned tubes to new ozone safe refrigerants and low boiling hydrocarbons has been investigated at our laboratory during the past years (c.f. /10/, /15/-/20/). In this chapter, the results with possible substitutes for R12 are summarized, cf. Table II. The test tubes used were a plain copper tube with 8mm outer diameter and three finned tubes with different fin shapes and approx. 15 mm outer diameters. One had the well known trapezoid-shaped fins, but with smaller fin distances than in the past (36 fins per inch: tube K36), the fins of the others were partly flattened, and a T-shaped (TX tube, 19 fins per inch) or Y-shaped (YX tube, 26 fins per inch) cross section of the fins is achieved, producing channels with narrow gaps on top of the fins, cf. Table II. For further enhancement of the nucleate boiling heat transfer, small cavities were milled in the tube surfaces at the bottom of the channels between the fins.

In the case of the finned tubes, the superheat ΔT of the tube wall in eq(1) is defined by

$$\Delta T = T_{Wall,\,core} - T_S \qquad (1a).$$

$T_{Wall,\,core}$ is the temperature at the bottom of the fins (taken constant throughout the tube length), so α contains the resistance against heat transfer from the tube surface to the boiling liquid, together with the resistance by heat conduction within the fins. (Calculations have shown, however, that conduction in the fins may be neglected with copper as wall material /17/). The overall limit of error of the heat transfer coefficient α is approx. 3 % at high wall superheats ΔT (high heat fluxes and small saturation pressures, cf. eg. Fig. 4, on the right) and is approx. 20% at small wall superheats ΔT (small heat fluxes and high saturation pressures) /2/.

TABLE II: Survey of test tubes (copper) and test liquids

test tubes	K35 (φ = 3.51) 36 fins/inch	TX19 (φ = 3.51) 19 fins/inch	YX26 (φ = 3.95 26 fins/inch	plain (φ = 1) –
fin shapes (to scale)	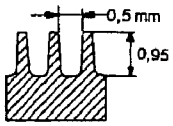	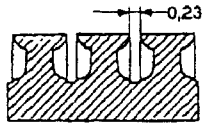	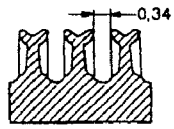	
test liquids				
Propane (C_3H_8)	*	*	*	*
R227 ($CF_3.CHF.CF_3$)	*	*	*	*
R134a ($CH_2f.CF_3$)	*	*	*	*
R152a ($CH_3.CHF_2$)	*		*	*
R134a/152a	*			

$$\varphi = \frac{A}{A_K} = \frac{\text{surface area of finned tube}}{\text{surface area of the tube without fins } (= d_K \pi L)}$$

Manufacturer of the finned test tubes: Wieland-Werke AG, Ulm, Germany; trade name: GEWA-tubes

The diagrams of Fig.4 show part of the experimental results (for further data cf. /10/, /15/ - /19/). For the tube with ***traditional shape of the fins*** (diagrams on top of Fig. 4), the heat transfer coefficient α at nucleate boiling increases with rising heat flux and pressure in a similar way as for plain tubes, as is well known from tubes with wider fin distances, cf. eg. /11/. The data for R134a and R152a are nearly identical for this tube, and the α-values of the mixture are only very slightly inferior to the pure components (right hand diagram on top), because the two refrigerants form a very narrow boiling binary system with vapour and liquid compositions being not more than approx. two mole per cent apart, see Fig. 5 (cf. also /21/). Therefore, no significant deterioration of nucleate boiling heat transfer will take place.

For the tubes with ***special fin structures*** for enhanced heat transfer (middle and bottom diagrams), the increase of α with q and p_s tends to vanish at high heat fluxes and low normalized pressures p* (below approx. 20 per cent of the critical pressures), the effect being somewhat more pronounced with the TX tube than with the YX tube. Photographs of the bubble formation under these conditions (shown in /15/) reveal that

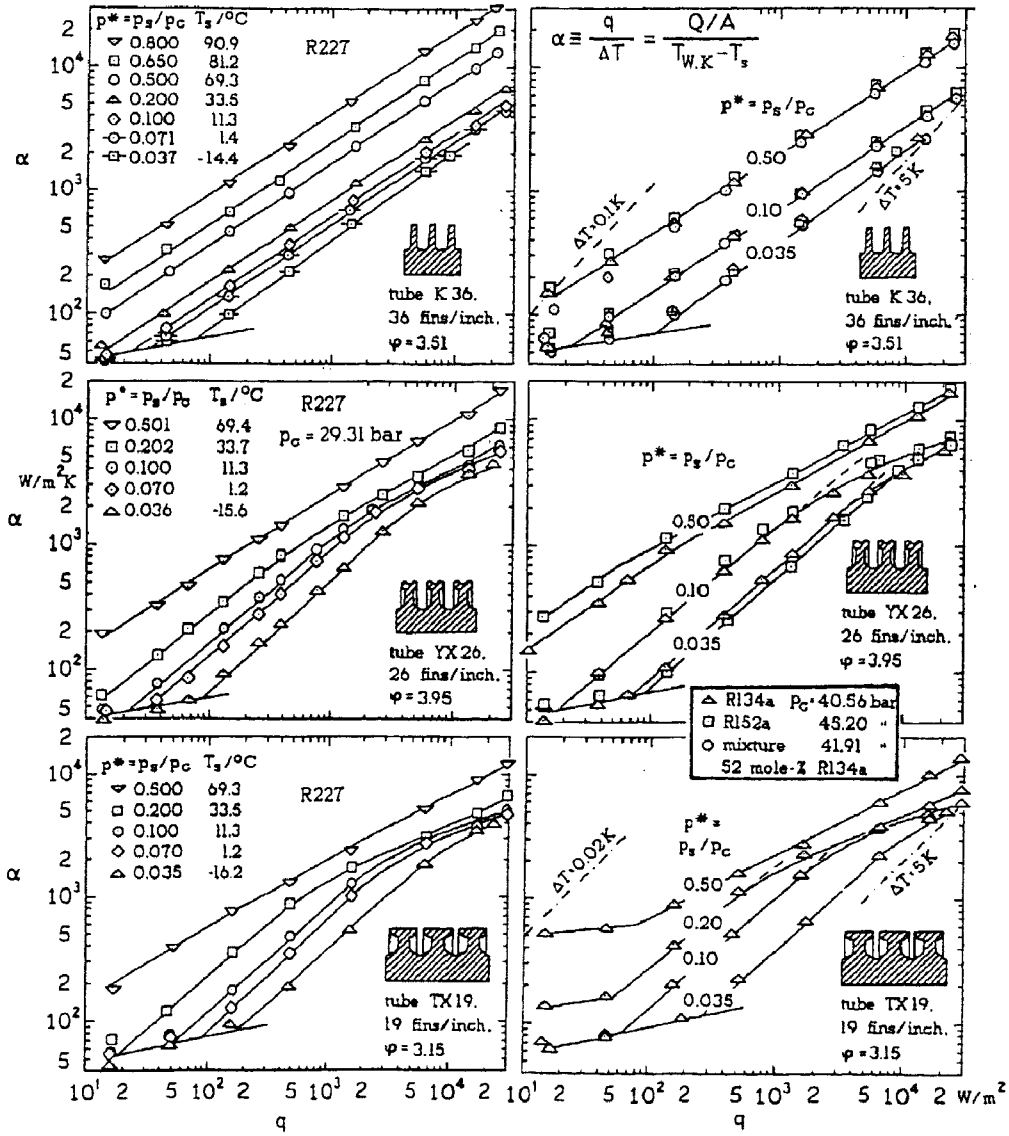

Fig.4: Double logarithmic plots of the heat transfer coefficient α over the heat flux q for pool boiling of various new refrigerants at the outside of three finned tubes with different shapes of the fins and similar relative augmentations φ of the outer surface.
Left hand side : R227($CF_3.CHF.CF_3$).
Right hand side: R134a($CH_2F.CF_3$), R152a($CH_3.CHF_2$), mixture.
Dot dashed straight lines: Constant excess temperature ΔT.

almost only big "secondary" bubbles, emerging from the gaps between the fins, detach from the tube, and that almost no active nucleation centers exist on the *outer* tube surface, despite the high heat fluxes. Consequently, this form of vapour release from the tube dominates heat transfer and results in "convective-like" heat transfer coefficients, being nearly independent of heat flux and pressure. The effect is less dominant with the YX tube, because the gaps between the fins are wider and the shape is better suited for convective vapour transport than with the TX tube (cf. Tab.II).

At very small heat fluxes and at saturation pressures above 10 per cent of the critical pressure, the data of the TX tube for R134a (and for all the other liquids investigated, except R227) exhibit a second special feature with α-values much higher than expected and nearly independent of heat flux (diagram at the bottom of Fig.4, on the right). This is caused by "trapping" the vapour between the fins on top of the tube (cf. the photographs in /15/) and by evaporative cooling of the superheated liquid streaming upwards, at the vapour-liquid interphase of the trapped vapour.

In Fig.6, the mutual comparison of the results for the different finned tubes as well as the comparison with the plain are shown at a constant, intermediate heat flux $q_K = \varphi \cdot q = 20\,000$ W/m^2 (corresponding to $5\,000 < q < 6\,000$ W/m^2, cf. "φ" in Table II). As can be seen, the tube with the YX-structure ist best (rhombs) with up to four times higher α-values than for the plain (triangles) between 3 and 10 per cent of the critical pressure. It is followed by the TX tube (squares) with roughly 30% lower α_K-values, and by the K tube (circles) which nearly equals the TX tube at $p^* \approx 0.03$ and $p^* \approx 0.2$.

While there are almost no differences between the α_K-values at constant *normalized* saturation pressure for propane, R134a, R152a and the mixture with the plain and the K tube, differences occur with the tubes with partly flattened fins, increasing from the TX to the YX tube. Comparing with the highly fluorinated refrigerant R227 (left hand diagram of Fig.6), the *relative* effects are the same as discussed above for the other substances, the *absolute* α_K-values at the same heat fluxes and normalized saturation pressures, however, being smaller than for the other substances, with decreasing differences from the YX tube to the plain (cf. also /18/).

The relative increases of the heat transfer coefficient with heat flux and normalized pressure p^* may be correlated by similar methods for the K tube with very small fin distances, but traditional fin shape, as for plain tubes, cf. /19/, /11/, /22/. These methods are not (yet) suited, however, to correlate the data of the tubes with YX-structure or TX-structure because of their $\alpha(q)$- or $\alpha(p^*)$-relationships which differ markedly from the plain or traditionally finned tubes, see Figs.4 and 6.

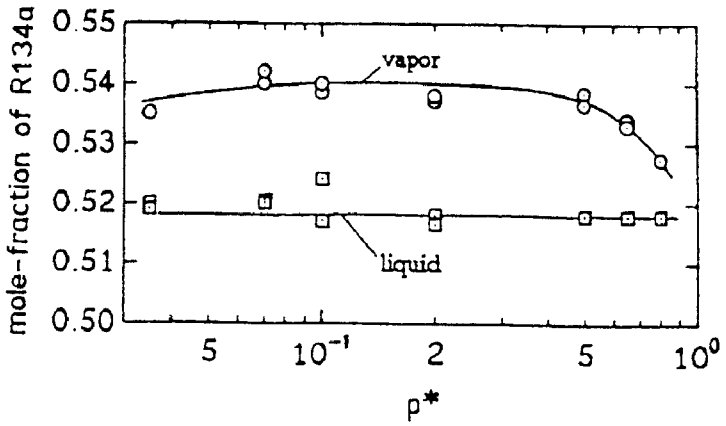

Fig.5: Mole fraction of the lower boiling component R134a in the vapour and liquid phase of the nearly equimolar mixture of R134a/R152a as functions of the normalized pressure $p^* = p_s/p_c$

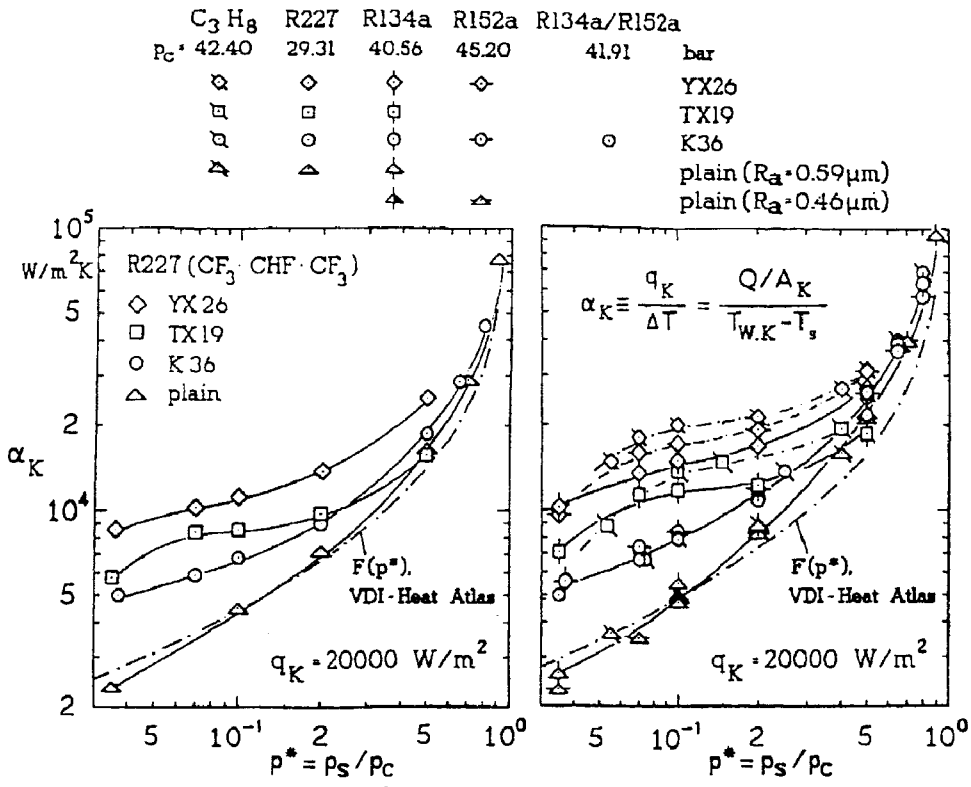

Fig.6: Comparison of the different finned tubes and the plain: Heat transfer coefficients $\alpha_K = \varphi \cdot \alpha$ as functions of the normalized saturation pressure p^* for various new refrigerants and propane at the constant heat flux $q_K = \varphi\, q = 20000\ W/m^2$

As to the ***overall heat transfer***, the improvement by the finned tubes will be less than demonstrated by Fig.6 when heated by a liquid flowing inside the tubes, unless the heat transfer *within the finned tubes* has been improved, too. Furthermore, one has to mind in the entire comparison of the results, that the tubes were tested with different surface roughnesses: the finned as coming from production, the plain after being treated with emery paper (cf. the R_a-values in Fig.6 and /17/). This does not affect the comparison with regard to practical use, because commercially available tubes will hold similar roughness values. For correct interpretation of the various reasons for enhanced nucleate boiling heat transfer with finned tubes, however, it will be necessary to investigate plain and finned tubes with the *same* surface roughness.

4 CONVECTIVE EFFECTS ON POOL BOILING HEAT TRANSFER WITHIN TUBE BUNDLES

The convective heat transfer caused by vapour bubbles and liquid streaming upwards within the bundle of a shell-and-tube evaporator has been simulated by a single tube with big diameter and devices for the additional flow of liquid or vapour from below. The big diameter of D = 88.4 mm was chosen in order to get clear evidence of variations of the local heat transfer along the circumference of the tube. Sectional views of the test tube and its position within the evaporator vessel are shown in Fig.7. The tube consists of an inner copper tube and two mild steel tubes soldered together on their entire heated length of 192.4 mm. The inner tube bears 40 resistance heaters in equidistant, longitudinal grooves, the middle 26 thermocouples of 0.5 mm diameter, 20 of which are placed on the front side of the tube to combine the observation of the bubble formation with local temperature readings during the measurements. (Former version of the test tube: 30 heaters, 17 thermocouples, 190 mm heated length, D = 88.9 mm). A U-shaped horizontal heater and a distributing tube for liquid are mounted 50 mm below the test tube, simulating bubbly flow by heat flow rates Q up to 6220 W per metre test tube length or liquid flow up to 43 litres per metre test tube length, resp. .

The boiling liquids investigated are given in Table III. Besides the pure hydrocarbons two binary mixtures have been chosen, because the well known deterioration of heat transfer with mixtures compared to the pure components should be reduced by additional flow of vapour or liquid. The pressure was varied between 10 and 50% of the critical pressures (the critical pressures of the mixtures were taken from /23/), resulting in variations of the saturation temperature T_s between -3°C and 111°C. The composition x of the liquid in the evaporator varied due to the shift of different amounts of the components from the evaporator vessel to other parts of the test loop. The x-data were taken at q = 20 000 W/m^2 and equilibrium conditions of the pool in the evaporator.

The effect of additional flow of bubbles on the heat transfer coefficient α at different heat inputs Q to the supplementary heater is shown in Fig.8 on top, with the 25/75 mole % propane/n-butane mixture at a pressure of p* = 0.2 as an example. As can be seen, the α-values without additional flow (closed rhombs) have been increased very significantly by the additional bubbles for small heat fluxes q at the test tube surface (open symbols). At q = 100 W/m^2, the effect amounts roughly to a factor of six for the smallest heat input Q represented (triangles). A further increase of Q by 350%, however, causes α to increase by not more than 25% (squares). In analogy to forced convective boiling within tubes at small heat fluxes, the heat transfer coefficient is independent of q and is dominated by the (three different) amounts of bubbles streaming to the tube. With increasing heat flux, a transition zone is beginning, and at fully developed nucleate boiling - q > 20 000 W/m^2 - the effect has vanished.

The lower diagram of Fig.8 demonstrates the influence of the saturation pressure for the equimolar mixture and the intermediate heat input Q = 3 050 W/m of the upper diagram. The marked increase of α with the saturation pressure, characteristic for nucleate boiling,

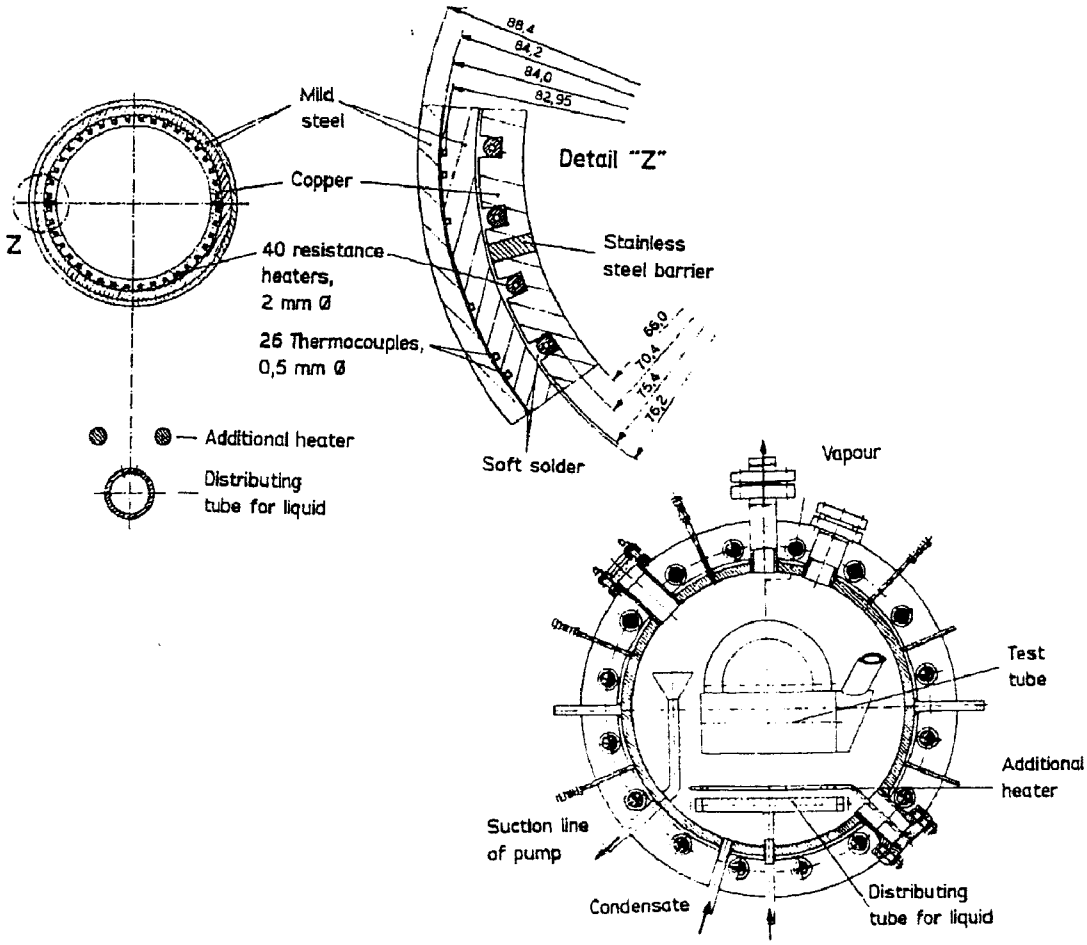

Fig.7: Sectional views of the test tube with 88.4 mm O.D. (top) and of the evaporator vessel (bottom). Below the test tube: U-shaped heater and distributing tube for additional flow of bubbles or liquid from below.

does not exist within the convective domain, like at natural convection without bubble formation. Instead, the α-values decrease slightly with increasing pressure and the beginning of the transition zone (dashed) is shifted to lower heat fluxes; the end, however, is nearly independent of pressure.

The comparison of the results for the mixtures (triangles) and the pure components (circles and squares) is represented in the two diagrams of Fig.9. They reveal for the domain ***dominated by convection***:

a) At constant normalized pressure p*, the heat transfer coefficients for the two pure components (circles and squares with dashes) coincide within the experimental limit of error; the same holds for the mixtures (triangles with dashes).

b) At p* = 0.1, the α-values for the mixtures are the same as for the pure components or but very slightly inferior (upper diagram), whereas this difference increases with rising pressure and amounts to approx. -20% at p* = 0.5. As the supplementary heater is operated at high heat fluxes, this decrease is an effect of less *relative* vapour production in the case of the mixtures at the same heat input as with the pure components because of the marked deterioration of heat transfer at the supplementary heater (compare triangles and circles/squares without additional bubbles at high heat fluxes and p* = 0.5).

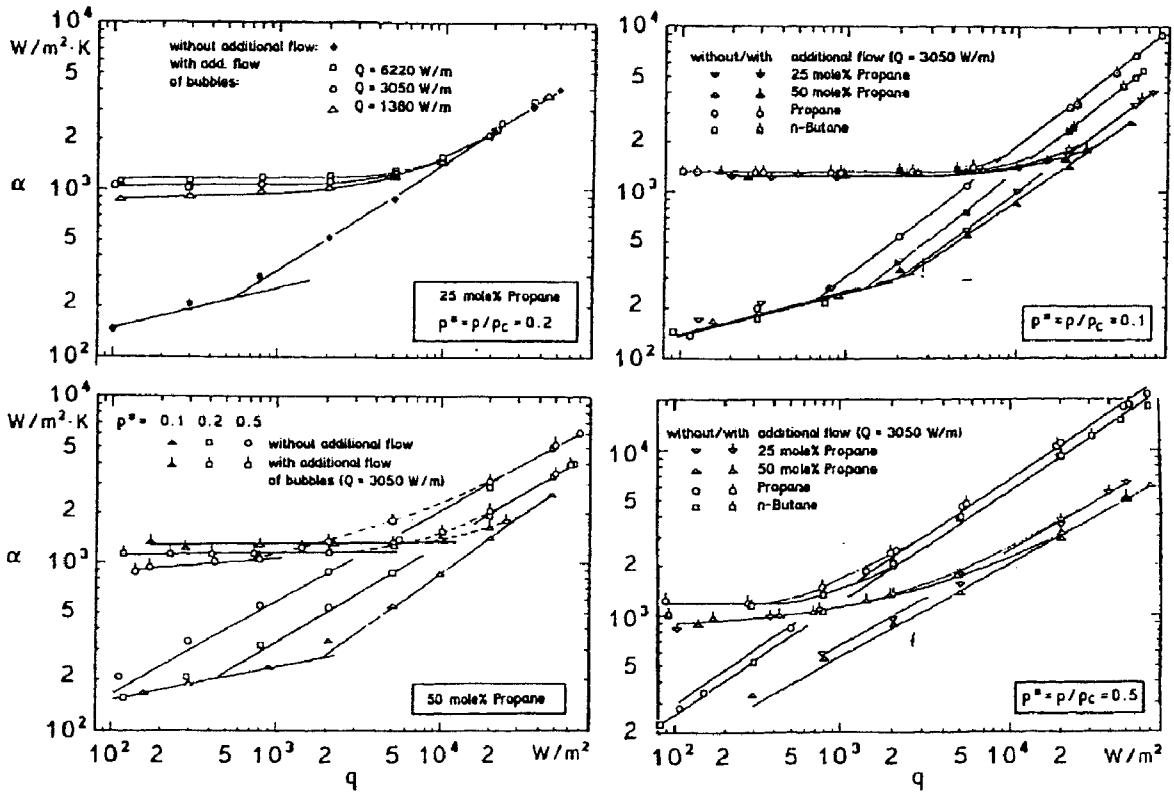

Figure 8 (left hand side): Heat transfer coefficient α as function of the heat flux q for boiling of propane / n-butane mixtures with and without additional flow of bubbles.
Top : Variation of the heat input Q (per metre test tube length) to the additional heater.
Bottom: Variation of the normalized pressure p* at constant heat input Q = 3 050 W/m.

Figure 9 (right hand side):
Heat transfer coefficient α as function of the heat flux q for boiling of two propane/ n-butane mixtures and for the pure components with and without additional flow of bubbles at constant heat input Q = 3 050 W/m to the additional heater. Top : p* = 0.1; Bottom: p* = 0.5. Closed symbols in the upper diagram: Conditions for the data of Fig.10.

c) The convective domains and the transition zones extend to higher heat fluxes with the mixtures than with the pure components. Thus, beginning at approximately 20 000 W/m^2, the deterioration of heat transfer without additional flow of bubbles is partly compensated and finally more than fully compensated at small heat fluxes. Only at very intense nucleate boiling with dense populations of growing bubbles on the heated surface, the additional bubbles are not favourable to heat transfer any more.

In the following, the effect of the additional bubbles will be analyzed in detail by means of the circumferential variation of the local superheat ΔT of the tube surface at $p^* = 0.1$ and three heat fluxes of 2000, 5 000 and 20 000 W/m^2, with the equimolar mixture and pure n-butane as examples (cf. the closed symbols in Fig.9 on top). In Fig.10, ΔT is plotted over the circumferential angle φ, with zero on top of the tube. Each measuring point has been transformed to the opposite tube side by a cross (+), thus the shapes of the curves appear more distinctly.

Results without additional bubbles (squares): The smallest superheats occur at the flanks where the bubbles produced on the lower parts of the tube are sliding upwards along the tube surface and enhance heat transfer compared to the bottom or top, resp.. The *relative* differences of ΔT between bottom, top and flanks of the tube are the same with the pure fluid and the mixture, the *amount* of the superheat, however, is always higher with the mixture.

Results with additional bubbles (triangles): The additional bubbles improve the heat transfer most at the bottom of the tube, where they reach the tube wall, produce additional convection and provide supplementary vapour interface for the superheated liquid to evaporate. Thus, the minima of ΔT are shifted to the bottom of the tube. The differences between the pure component and the mixture have almost vanished at the two lower fluxes (lower diagrams of Fig.10), the superheats of the mixture being only very slightly higher, all over the tube surface. At the *high flux*, the additional bubbles reduce the superheat for the boiling *mixture* by approx. 20 % at the bottom and 10 % at the flanks and the

TABLE III: Critical pressures p_c and temperatures T_c, saturated states and compositions of the liquids investigated

		Propane C_3H_8	Butane $n\text{-}C_4H_{10}$	mixture 1 "25 mole %"	mixture 2 "50 mole %"
purity	vol.-%	>99.5	>99.5		
critical	p_c/bar	42.64	37.96	(viz. "saturated	
data	T_c/°C	96.84	152.01	state")	
saturated state 1	p_s/bar	4.36	3.79	4.07	4.25
$p^* = p_s/p_c = 0.1$	T_s/°C	-3.02	39.98	24.45	13.43
	x/mole %[1)]			22.1	45.2
	p_c/bar			40.2	41.85
saturated state 2	p_s/bar	8.48	7.59	8.14	8.48
$p^* = 0.2$	T_s/°C	20.46	67.27	51.30	41.88
	x/mole %[1)]			23.6	45.8
	p_c/bar			40.25	41.9
saturated state 3	p_s/bar	21.21	18.90	20.35	21.11
$p^* = 0.5$	T_s/°C	60.05	111.22	96.16	84.33
	x/mole %[1)]			27.3	48.7
	p_c/bar			40.6	42.1

1) The composition x of the liquid in the evaporator varied due to the shift of different amounts of the components to various parts of the test loop. The x-data were taken at q = 20 000 W/m^2 and equilibrium conditions of the pool in the evaporator.

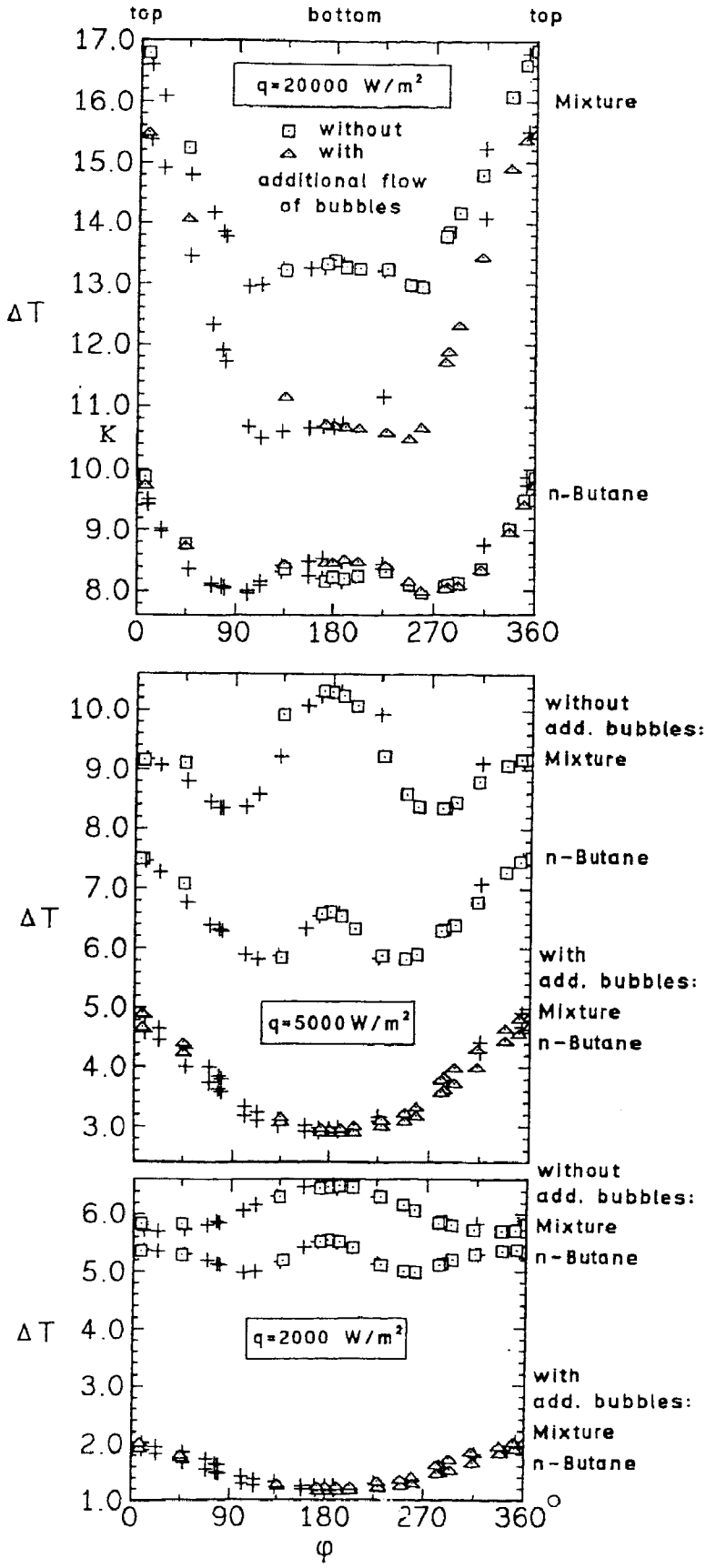

Fig.10: Local superheat ΔT of the tube surface as function of the circumferential angle φ for pure n-butane and the mixture with 50 mole% propane at the measuring conditions indicated by full symbols in Fig.9, top.
Top: Heat flux q = 20 000 W/m²; middle: q = 5 000 W/m²; bottom: q = 2 000 W/m².

top of the tube (upper rows of points in the upper diagram of Fig.10). For butane, however, it can be seen that the local superheats *increase* slightly by the additional bubbles at the bottom of the tube. Obviously, a dense layer of bubbles is already produced by nucleate boiling at this heat flux, and the additional bubbles merely cause a (slight) additional resistance for the transport of liquid to the tube surface. Whereas at the upper parts of the tube, this effect is compensated by enhanced convection.

Figure 11 shows one example of the results *with additional flow of liquid*, the increase of the heat transfer coefficient and the relative effects discussed for the mixtures and the pure components being quite similar as with the additional flow of bubbles.

At present, a third propane / n-butane mixture is being investigated experimentally, and the results for propane and n-hexane with additional flow of bubbles are compared with a calculation method for the heat transfer coefficient *within the convective domain* developed by Fujita et al /24/. As the additional heater simulates a second tube at a comparatively large distance (s = 2 D, cf. Fig.12), a modification of the original calculation has been applied, proposed for this case by Windisch /25/. Furthermore, the saturation pressure p_s was replaced by the normalized pressure $p^* = p_s / p_c$ in an empirical correlation derived in /24/ from experiments with R113 between 1 and 10 bar ($0.029 \leq p^* \leq 0.29$), in order to apply it for other liquids,

$$\alpha_{Konv} = 7\,000\,(V/k)^{0.22p^{-0.18}} \quad \rightarrow \quad \alpha_{Konv} = 7\,000\,(V/k)^{0.177p^{*-0.18}} \qquad (6),$$

with V = volume of the vapour streaming upwards, and k giving the ratio of the enthalpy of the vapour produced over the total heat input to the additional heater or the tube below, resp..

The comparison of measured data (symbols) with calculated results (lines) is represented in Fig.13. (The index "2" at the heat transfer coefficient indicating the second tube in a vertical row). As can be seen, the measurements agree very well with the calculated lines for the plain tube and constant pressure in the upper diagram, as well as for a finned tube with similar big diameter (D = 101.2 mm) and constant heat input Q to the additional heater in the lower - despite the fact that the pressure range of eq (6) has been extra-

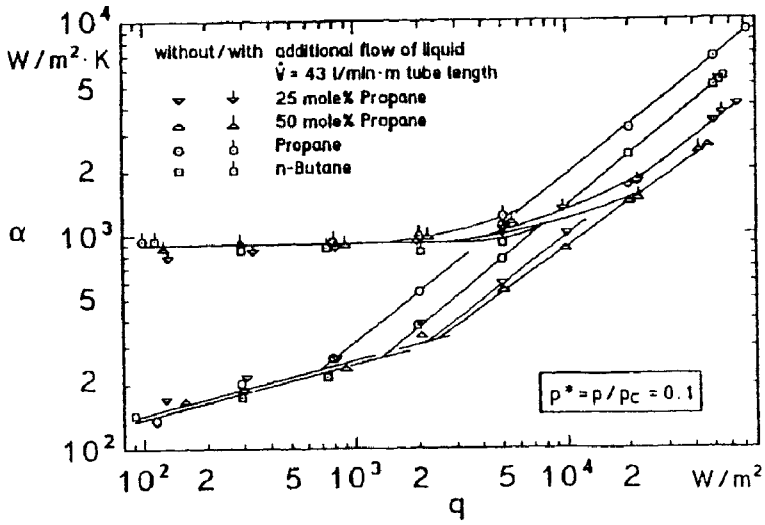

Fig.11: Heat transfer coefficient α as function of the heat flux q for boiling of two propane/n-butane mixtures and for the pure components with and without additional flow of liquid at constant pressure p* = 0.1 and constant output of the liquid pump (43 litres per minute and metre of test tube length).

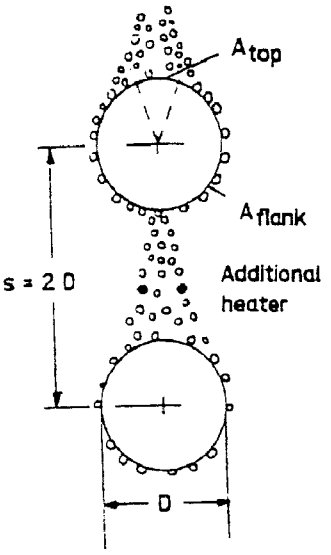

Fig. 12: Bubbles rising from a tube below the test tube, simulated by the additional heater.

polated. Some of the original data of Fujita et al for a plain tube with D = 25 mm and R113 have been added as squares or rhombs demonstrating the similar behaviour of this former refrigerant.

Acknowledgement

The results presented in this review are taken from the doctoral theses of Martin Buschmeier, Socrates Caplanis, Admilson Dultra Pinto, Wolfgang Künstler, Andrea Luke and Peter Sokol, which are actually in progress.

REFERENCES

/1/ Gorenflo, D., J. Goetz and K. Bier: Vorschlag für eine Standard-Apparatur zur Messung des Wärmeübergangs beim Blasensieden. Wärme- und Stoffübertragung 16 (1982), 69 - 78; cf. also: J. Goetz, Diss. Universität Karlsruhe (TH), 1980.

/2/ Gorenflo, D. and W. Fath : Heat transfer on the outside of finned tubes at high saturation pressures. Proc XVIIth Int. Congr. Refrig., Vienna, 1987, Vol. B, 955 - 960; cf. also: W. Fath, Diss. Universität (GH) Paderborn, 1986.

/3/ Lance, R. P., J. E. Myers : Local boiling coefficients on a horizontal tube. AIChE J. 4 (1950), 75 - 80.

/4/ Bier, K., J. Goetz and D. Gorenflo : Zum Einfluß des Umfangswinkels auf den Wärmeübergang beim Blasensieden an horizontalen Rohren. Wärme- und Stoffübertragung 15 (1981), 159 - 169.

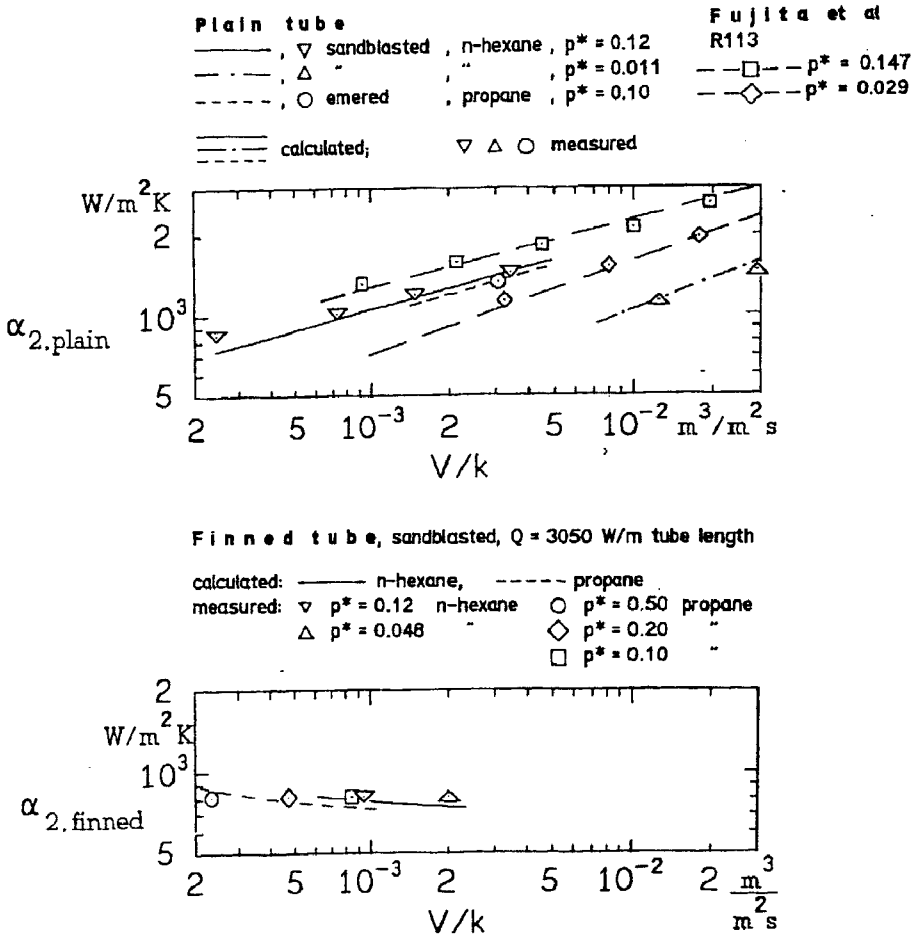

Fig. 13: Heat transfer coefficient α_2 at the upper tube of the arrangement of Fig. 12 as function of the upstreaming vapour volume V/k. Symbols : Measuring points. Lines : Calculated according to Fujita et al /24/. Top : Plain tube, D = 88 mm. Bottom : Finned tube, material: mild steel (St35.8); outer diameter 101.2 mm, fin height 6.15 mm, fin distance 3.75 mm.
For comparison: Data of /24/ for R113, copper tube, D = 25 mm: $\alpha = \alpha_{flank}$

/5/ Siebert, M. : Untersuchung zum Einfluß des Wandmaterials und des Rohrdurchmessers auf den Wärmeübergang von horizontalen Rohren an siedende Flüssigkeiten. Diss. Universität Karlsruhe (TH), 1987.

/6/ Cornwell, K., Schüller, R.B. and Einarsson, J.G.: The influence of tube diameter on nucleate boiling outside tubes. Heat Transfer 1982: Proc. 7th Int. Heat Transfer Conf., München 1982, Vol.4, 47-53.

/7/ Cornwell, K. and Einarsson, J.G.: Peripheral variation of heat transfer under pool boiling on tubes. Int. J. Heat Fluid Flow 4 (1983), 141-144.

/8/ Cornwell, K. and Einarsson J.G.: The influence of fluid flow on nucleate boiling from a tube. Exp. Heat Transfer 3 (1990), 101-116.

/9/ Cornwell, K.: The influence of bubbly flow on boiling from a tube in a bundle. Int. J. Heat Mass Transfer 33 (1990), 2579-2584.

/10/ Gorenflo, D., P. Sokol and S. Caplanis : Pool boiling heat transfer from single plain tubes to various hydrocarbons. Int. J. Refrig. 13 (1990), 286 - 292.

/11/ Gorenflo, D. : VDI-Heat Atlas. Chapter Ha: Pool boiling. VDI-Verlag Düsseldorf, 1993. English Version of 6th German ed., 1991.

/12/ Hahne, E., J. Shen, K. Spindler : Nucleate boiling at a thin Pt-wire. Unpublished measurements at the Institut für Thermodynamik u. Wärmetechnik, Universität Stuttgart, Nov. 1993.

/13/ Shi, K., E. Hahne and U. Gross : Pool boiling heat transfer in HFC - 134a, HFC - 152a and their mixtures. Proc. 18th Int. Congr. Refrigeration, Montréal 1991, Vol. II, 459 - 463.

/14/ Gorenflo, D. : VDI-Wärmeatlas. Kapitel Hab:Behältersieden. 7. Aufl. VDI-Verlag Düsseldorf, 1994.

/15/ Sokol, P., P. Blein, D. Gorenflo, H. Schömann : Pool boiling heat transfer from plain and finned tubes to Propane and Propylene. Heat Transfer 1990: Proc. 9th Int. Heat Transfer Conf., Jerusalem 1990, Vol. 2, 75 - 80.

/16/ Gorenflo, D., P. Blein, S. Caplanis, P. Sokol : Pool boiling heat transfer from a GEWA-TX finned tube to low boiling hydrocarbons. In: Progress in the science and technology of refrigeration in food engineering. Internat. Inst. Refrig., 1990-4, 249 - 256.

/17/ Gorenflo, D., P. Sokol, S. Caplanis : Pool boiling heat transfer from single tubes to new refrigerants. Proc. 18th Int. Congr. Refrigeration, Montréal 1991, Vol.II, 423 - 428.

/18/ Gorenflo, D., P. Sokol, S. Caplanis : Zum Wärmeübergang beim Blasensieden von Kohlenwasserstoffen und Halogen-Kältemitteln an einem Glattrohr und einem Hochleistungs-Rippenrohr. Wärme- und Stoffübertragung 26 (1991), 273 - 281.

/19/ Gorenflo, D., P. Sokol, S. Caplanis : Measurements of enhanced pool boiling heat transfer. 1st European Conf. on Thermal Sciences, Birmingham 1992, Vol. 1, 89 - 96.

/20/ Gorenflo, D., S. Caplanis, W. Künstler : Enhanced pool boiling heat transfer to new refrigerants. In: Energy efficiency in refrigeration and global warming impact. Int. Inst. Refrig., 1993-2, 327 - 334.

/21/ Bier, K., M. Nagel, J. Zhai: Phasengleichgewichte und kritische Zustände neuer Kältemittel und Kältemittelgemische. DKV-Tagungsbericht 19 (1992), Bd.II.1, 121-152

/22/ Slipčević, B.: Wärmeübertragung bei Verdampfung in natürlicher Strömung und Bemessung von überfluteten Verdampfern. In: Handbuch der Kältetechnik, Vol. VI B, R. Plank, F. Steimle, K. Stephan ed., Springer Verlag Berlin, 1988, 76 - 152.

/23/ Bednar, W., K. Bier: Wärmeübergang beim Behältersieden von Propan/n-Butan-Gemischen. DKV-Tagungsbericht 20 (1993), Bd. II.1 in press; cf. also: W. Bednar, Diss. Universität Karlsruhe (TH), 1993.

/24/ Fujita, Y., H. Ohta, S. Hidaka, K. Nishikawa: Nucleate boiling heat transfer on horizontal tubes in bundles. Proc. 8th Int. Heat Transfer Conf., San Francisco 1986, Vol. 5, 2131 - 2136.

/25/ Windisch, R.: Wärmeübergang beim Sieden von Kältemitteln an Einzelrohren, Zweirohranordnungen und Rohrbündeln. Diss., Universität Stuttgart, 1988.